Voltage- and time-dependent properties of the recombinant rat vanilloid receptor (rVR1)

Martin J. Gunthorpe, Mark H. Harries, Rab K. Prinjha, John B. Davis and Andrew Randall

Neuroscience Research, SmithKline Beecham Pharmaceuticals, New Frontiers Science Park (North), Harlow, Essex CM19 5AW, UK

(Received 2 February 2000; accepted after revision 28 March 2000)

1. Whole-cell voltage-clamp techniques were used to investigate the capsaicin-, voltage- and time-dependent properties of the rat vanilloid receptor (rVR1) stably expressed in human embryonic kidney (HEK) 293 cells.

2. At a holding potential of −70 mV, application of capsaicin (0·03–30 μM) to HEK 293 cells expressing the rVR1 receptor led to the appearance of inward currents (EC_{50}, 497 nM; Hill coefficient, n_H, 2·85) which were reversibly antagonized by 10 μM capsazepine.

3. Current–voltage relationships, determined using depolarizing or hyperpolarizing voltage ramps, had reversal potentials close to 0 mV, exhibited substantial outward rectification and possessed a region of negative slope conductance at holding potentials negative to around −70 mV. Further experiments indicated that the outward rectification and the region of negative slope conductance did not result from external block of the channel by either Ba^{2+}, Ca^{2+} or Mg^{2+}.

4. During our characterization of rVR1, it became apparent that the rectification behaviour of this receptor was not entirely instantaneous as might be expected for a ligand-gated ion channel, but rather displayed clear time-dependent components. We characterized the kinetics of these novel gating properties in a series of additional voltage-step experiments.

5. The time-dependent changes in rVR1-mediated conductance due to membrane depolarization or repolarization occurred with bi-exponential kinetics. On depolarization to +70 mV the time-dependent increase in outward current developed with mean time constants of $6{\cdot}7 \pm 0{\cdot}7$ and $51{\cdot}8 \pm 18{\cdot}4$ ms, with the faster time constant playing a dominant role ($64{\cdot}4 \pm 3{\cdot}8$ %). Similar kinetics also described the decay of 'tail currents' observed on repolarization. Furthermore, these time-dependent changes appeared to be unaffected by the removal of extracellular divalent cations and were not significantly voltage dependent.

6. Our data reveal that rVR1 exhibits substantial time- and voltage-dependent gating properties that may have significance for the physiology of sensory transduction of nociceptive signals.

Current rectification is a common property of both ligand- and voltage-gated ion channels (Hille, 1992). There are many good examples of the physiological importance of the rectification process. Specifically with regard to the nervous system, early studies highlighted the doubly rectifying channels at electrical synapses in invertebrates, which allow excellent bidirectional communication of depolarization but poor transmission of hyperpolarization (Baylor & Nicholls, 1969; Acklin, 1988). More recent work has uncovered the pivotal role of NMDA receptor rectification in synaptic integration and plasticity (Collingridge & Watkins, 1994).

Current rectification can occur for any of several reasons. In its simplest form, rectification arises from the unequal distribution of permeant species across the lipid bilayer (Goldman, 1943; Hodgkin & Katz, 1949). Voltage dependence of the probability of channel opening is also a common source of macroscopic current rectification commonly responsible for the current–voltage properties of voltage-gated channels. In other instances, voltage-dependent block of channel activity by a physical entity can produce substantial current rectification and may even result in regions of negative slope conductance. Examples of this mechanism include the Mg^{2+} block of the NMDA receptor (Nowak *et al.* 1984) and the polyamine block of certain inwardly rectifying K^+ channels (Lopatin *et al.* 1994). The observation of rectification of single-channel currents under

simplified recording conditions, e.g. use of bi-ionic or symmetrical conditions, limits the possible sources of rectification and usually suggests a clear voltage dependence in the ion permeation pathway (Hille, 1992).

The pungent alkaloid capsaicin has long been known to produce substantial outwardly rectifying $Na^+/K^+/Ca^{2+}$-mediated current responses in voltage-clamped sensory neurones (Heyman & Rang, 1985; Marsh *et al.* 1987; Wood *et al.* 1988; Bevan & Szolcsanyi, 1990; Oh *et al.* 1996; Zeilhofer *et al.* 1997). Recently the receptor responsible for this activity was cloned from rat tissue (Caterina *et al.* 1997). It was named the vanilloid receptor-1 (VR1) after its ability to respond to a range of vanilloid moieties including capsaicin itself. Heterologous expression of the rat vanilloid receptor (rVR1) has revealed that in addition to capsaicin-mediated activation, it also acts as a polymodal sensory detector, being capable of responding to both changes in pH and temperature (Tominaga *et al.* 1998). Whether activated chemically, by H^+, or by heat, responses mediated by recombinant rVR1 exhibit substantial outward rectification (Caterina *et al.* 1997; Tominaga *et al.* 1998), and thus resemble the responses elicited by capsaicin or heat in sensory neurones (Oh *et al.* 1996; Piper *et al.* 1999; Nagy & Rang, 1999). Initial single-channel studies of rVR1 indicate that these rectification properties may extend to the single-channel level, thus ruling out a number of possible mechanisms for their generation (Caterina *et al.* 1997; Tominaga *et al.* 1998; Nagy & Rang, 1999).

In this study we have characterized the capsaicin-, voltage- and time-dependent properties of the rVR1 receptor expressed in HEK 293 cells. Although our findings concerning the basic properties of rVR1 agree broadly with previous reports (Caterina *et al.* 1997; Tominaga *et al.* 1998) our results concerning the voltage-dependent properties of rVR1 differ in that they demonstrate that the rectification properties of rVR1 are time dependent. We have shown that the pronounced outward rectification properties of the receptor are not instantaneous – they are relatively slow to develop and recover in response to changes in membrane potential. To our knowledge, these time-dependent properties represent a novel finding for a ligand-gated ion channel and suggest that coincident action potential firing may serve to facilitate rVR1 activity *in vivo*.

METHODS

Cloning of rat VR1

Rat VR1 (rVR1) was cloned from total RNA prepared from L4 and L5 dorsal root ganglia (DRG) taken from lean adult LN/ZDF rats (3–4 months old). Animals were killed by exposure to a slowly rising concentration of CO_2 gas, according to the UK Animals (Scientific Procedures) Act of 1986 and approved by the SmithKline Beecham UK Procedures Review Panel. Following dissection, ganglia were immediately snap frozen in liquid nitrogen. For cloning purposes, ganglia were homogenized in 1 ml Trizol (Life Technologies) using a Polytron homogenizer and processed according to the manufacturer's instructions. Total RNA (~2 μg) from rat DRG was reverse transcribed using OligodT and Superscript reverse transcriptase (Life Technologies) at 42 °C. Reverse-transcription polymerase chain reactions (RT-PCR) were carried out with forward and reverse primers designed using the GenBank sequence AF029310 and which incorporated the restriction sites shown: rVR1F-*Hin*dIII (CATAAGCTTGCCGCCATGGAACAA-CGGGCTAGCTTAGACTCAGAGG) and rVR1R-*Xba*I (CATTCT-AGACCATTATTTCTCCCCTGGGACCATGG). One-tenth of the RT reaction was used in 100 μl PCR amplifications using Taq Plus Precision (Stratagene) according to the manufacturer's instructions. Reaction products were cloned into pBSIISK$^+$ (Stratagene), confirmed by sequencing and then subcloned into the *Hin*dIII–*Xba*I sites of pcDNA3.1 (Invitrogen). The accuracy of the entire open reading frame was then checked by DNA sequencing of both strands.

Cell culture

Human embryonic kidney (HEK) 293 cells were obtained from the European Collection of Animal Cell Cultures and cultured in modified Eagle's medium with Earle's salts, supplemented with 10% fetal calf serum, non-essential amino acids and glutamine, on plastic tissue culture grade dishes (Nunc). A stable clone expressing rVR1 was obtained by transfection of subconfluent HEK 293 cells using Lipofectamine Plus (Life Technologies) and rVR1.pcDNA3.1, according to the manufacturer's instructions, followed by selection in 400 μg ml^{-1} geneticin (Life Technologies) and colony cloning. Clones for further analysis were selected on the basis of mRNA expression levels, and functional rVR1 receptor expression was initially tested by examining capsaicin-induced increases in cytosolic calcium concentrations using fluo-4 calcium imaging. For electrophysiological recordings cells were plated onto glass coverslips coated with poly-L-lysine at a density of ~26 000 cells cm^{-2} and used after 16–48 h.

Solutions for electrophysiology

The bathing solution for most experiments consisted of (mM): NaCl, 130; KCl, 5; $BaCl_2$, 2; $MgCl_2$, 1; glucose, 30; Hepes–NaOH, 25; pH 7·3. In a few experiments equimolar Ca^{2+} was substituted for Ba^{2+} or divalent cations were omitted completely. The use of Ba^{2+} in most of our experiments was to reduce Ca^{2+}-dependent response rundown (Koplas *et al.* 1997). Electrodes were filled with (mM): CsCl, 140; $MgCl_2$, 4; EGTA, 10; Hepes–CsOH, 10; pH 7·3. Capsaicin (Calbiochem)-containing solutions were prepared from a 10 mM stock in dimethylsulphoxide. Drug applications were carried out using an automated fast-switching solution exchange system (Warner Instruments SF-77B). This device could perform individual solution changes in ~30 ms and was used to generate precisely timed applications of known doses of capsaicin.

Data acquisition and analysis

All recordings were performed at room temperature (20–24 °C) using standard whole-cell patch-clamp methods. Patch pipettes were fabricated on a horizontal electrode puller (Sutter Instruments P-87) and had resistances of 2–5 MΩ when filled with the electrode solution described above. Cells were visualized with standard phase-contrast optics and recordings were made from well isolated single phase-bright cells. Series resistance compensation was used where appropriate and averaged 71 ± 1% (n = 51). All data were recorded in voltage-clamp mode using an Axopatch 200B amplifier. This was controlled using the pCLAMP7 software suite, which was also used to acquire data to a personal computer. Curve fitting was carried out with either the Clampfit (Axon Instruments) or Origin (Microcal) software packages. In each case the goodness of fit was defined by the least squares method and all data are presented as the mean ± S.E.M., unless otherwise stated.

RESULTS

Activation of rVR1

Application of 30 μM capsaicin to HEK 293 cells stably expressing the rVR1 receptor led to the appearance of inward currents (at a holding potential of −70 mV) which recovered slowly to baseline levels on washout (Fig. 1). In contrast, no currents were detected in wild-type (parental) HEK 293 cells in response to 30 μM capsaicin ($n = 13$, data not shown). Dose–response relationships to capsaicin exhibited an EC_{50} of 497 ± 59 nM and a Hill coefficient of 2·85 ± 0·62 (Fig. 1; $n = 5$). Consistent with these data, 30 μM capsaicin was a supra-maximally effective agonist concentration, producing responses which averaged 662 ± 91 pA or 50·5 ± 7·0 pA pF^{-1} ($n = 23$), and these currents were reversibly antagonized by the VR1 antagonist capsazepine (10 μM; Fig. 1*C*; $n = 3$). In all, recordings were made from a total of 58 capsaicin-responsive cells; the mean membrane capacitance was 13·6 ± 0·6 pF and series resistance averaged 8·4 ± 0·4 MΩ.

Even at supra-maximal capsaicin concentrations, rVR1 responses took a number of seconds to reach peak current (Fig. 1*A* and *B*). For example, the 10–90% growth time for responses evoked by 30 μM capsaicin averaged 3·1 ± 0·2 s ($n = 7$, typical cells). Furthermore, the time course of recovery to baseline current after agonist removal was slow (typically > 20 s), and could not be fitted by a simple exponential function. Current activation was also consistently preceded by a significant delay of 405 ± 30 ms (see Fig. 1*B*; $n = 7$). These slow and somewhat complex activation and deactivation kinetics probably reflect the requirement of capsaicin to cross the plasma membrane in order to reach its binding site (Jung *et al.* 1999).

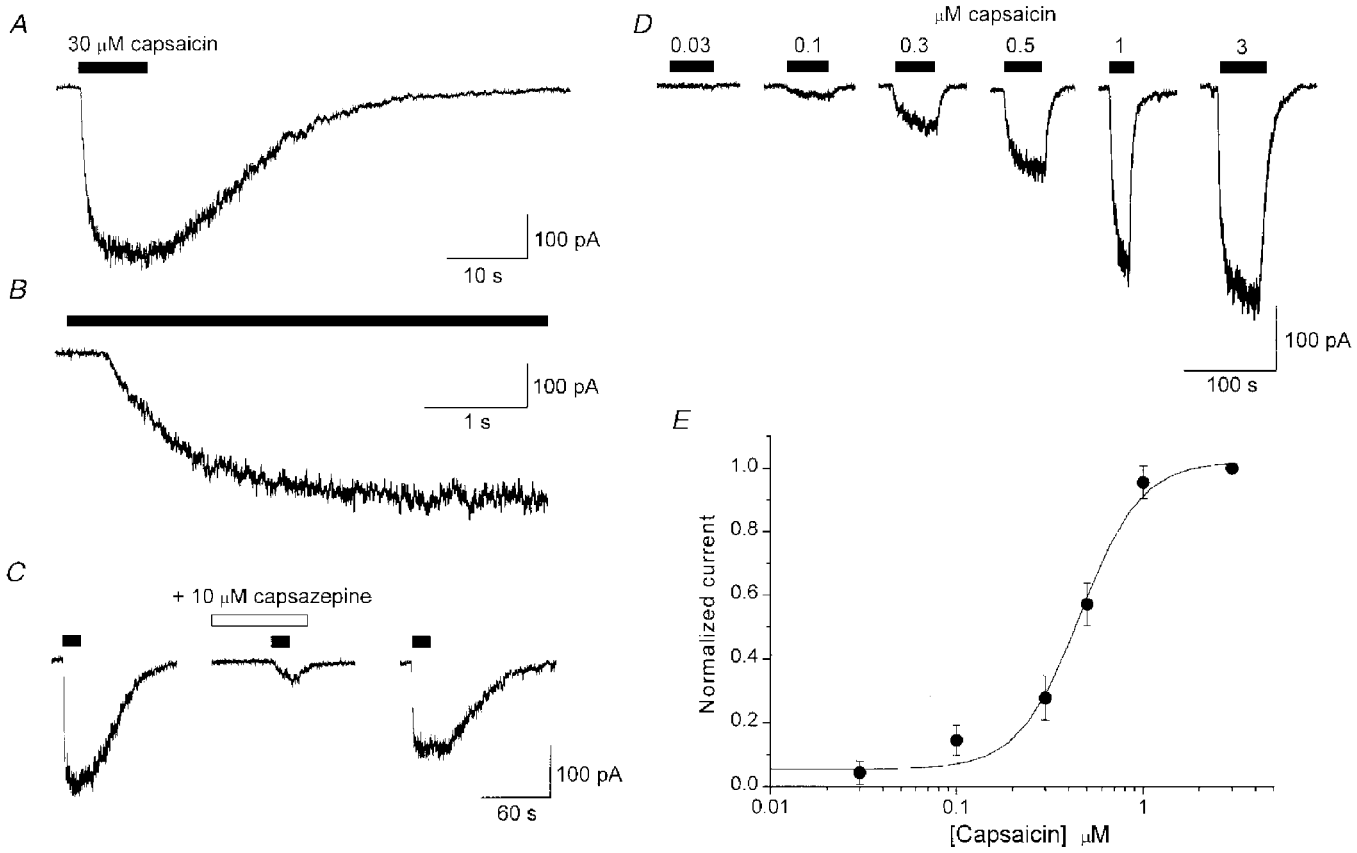

Figure 1. Activation of the rat vanilloid receptor (rVR1) expressed in HEK 293 cells by capsaicin

A, a typical whole-cell current response to the application of 30 μM capsaicin for the duration indicated by the filled bar (holding potential, −70 mV). *B*, expanded time course of the trace shown in *A* to highlight the significant time delay (405 ± 30 ms; $n = 7$) between capsaicin application and the onset of receptor activation. *C*, reversible antagonism of 30 μM capsaicin-gated currents by the competitive VR antagonist capsazepine (10 μM; $n = 3$). No currents in response to 30 μM capsaicin were detected in wild-type (parental) HEK 293 cells ($n = 13$). *D*, typical whole-cell current responses from experiments used to establish the dose–response relationship for rVR1 activation by capsaicin. The traces shown are from a single cell and are representative of five similar experiments in different cells. *E*, pooled, normalized, concentration–response data from five rVR1-expressing cells. The mean EC_{50} was 497 ± 59 nM and the Hill coefficient was 2·85 ± 0·62 ($n = 5$).

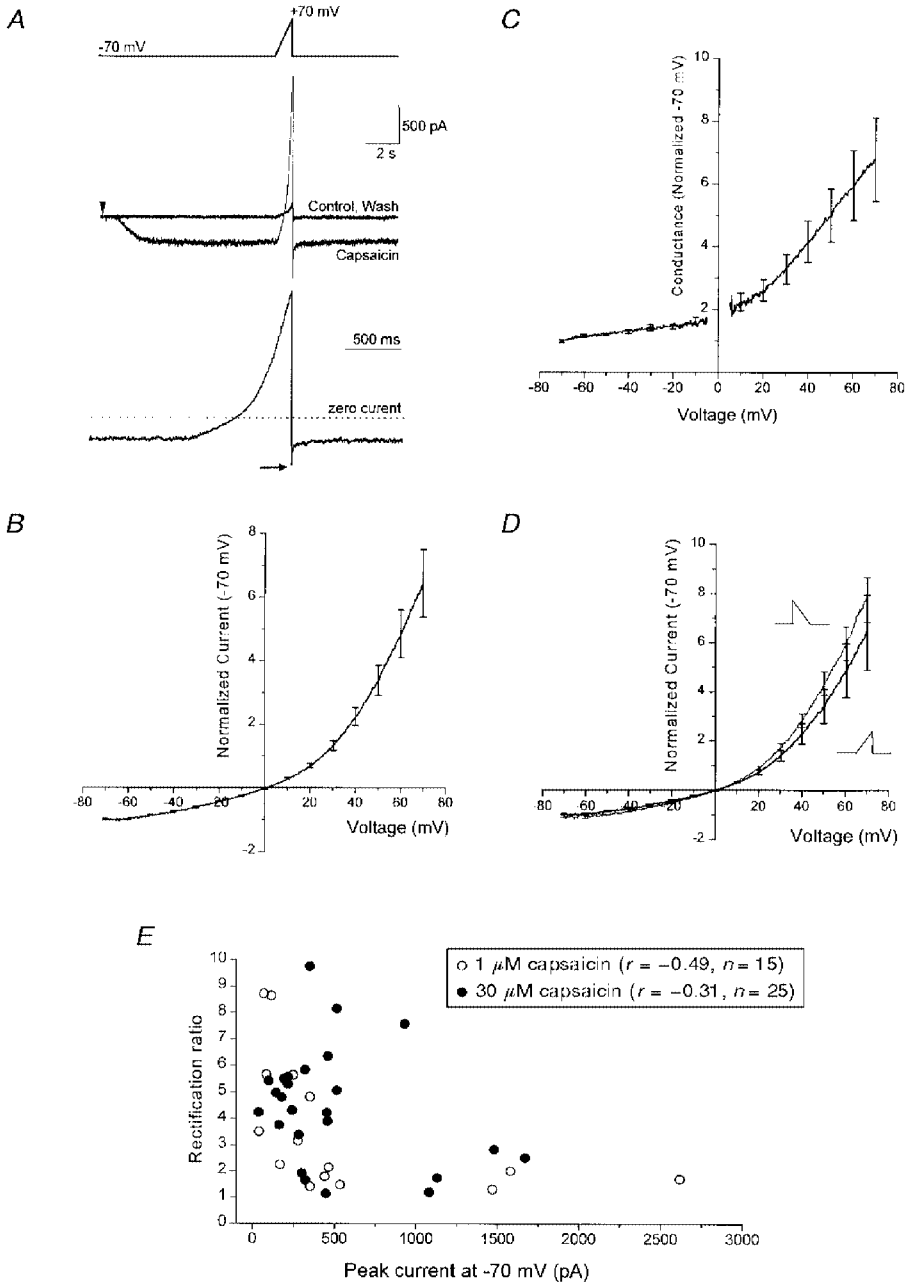

Figure 2. Voltage-dependent properties of capsaicin-gated rVR1 responses in HEK 293 cells

A, an example of a whole-cell recording illustrating the voltage-ramp protocol used to determine the current–voltage relationship of rVR1-mediated current. The upper panel outlines the voltage protocol which consists of a sustained period at −70 mV followed by a ramp to +70 mV applied at 0·14 mV ms^{-1}. The middle trace depicts three current traces which were collected in the following order: Control, Capsaicin, Wash. In the accordingly labelled trace capsaicin was applied at a concentration of 30 μM, from the time indicated by the arrowhead. This produced a slowly developing non-desensitizing current at −70 mV and a large outward current at +70 mV. Subtraction of the control current from that in which capsaicin was present was then used to produce the net capsaicin-gated current. In the lower panel, this is shown for the regions adjacent to and including the voltage ramp. Note the 'tail current' observed following the repolarization to −70 mV at the end of the voltage ramp (arrow). *B*, the mean current–voltage relationship determined from six voltage-ramp experiments including that shown in *A*. Prior to averaging across cells, data from each recording were normalized to the steady-state current observed at −70 mV. Occasional standard error bars from the averaging procedure are shown. *C*, the mean conductance–voltage relationship constructed from the same data shown in *B*. To produce this data set the conductance–voltage relationship was constructed from each individual cell using its measured reversal potential; this was then normalized to the steady-state conductance at −70 mV. Finally, the normalized conductance–voltage curves were averaged across all the cells to produce the relationship shown. *D*, comparison of current–voltage

Current rectification of capsaicin-gated rVR1 responses

Application of 1 or 30 μM capsaicin for periods as long as 30 s produced little or no macroscopic desensitization under the recording conditions employed (2 mM Ba^{2+} was used instead of 2 mM Ca^{2+}, see Methods; Figs 1*A* and 2*A*). This allowed us to study the voltage dependence of rVR1 receptor activity by applying voltage ramps and steps during the steady-state phase of the capsaicin-induced current responses.

In our first series of experiments to look at the voltage-dependent properties of rVR1 we characterized the voltage dependence of capsaicin-induced currents using a depolarizing voltage ramp. A typical recording from this series of experiments is shown in Fig. 2*A* (top). Here, an identical voltage ramp was applied before, during and following the application of 30 μM capsaicin. In the time between voltage ramps the cell was maintained at −70 mV, a potential at which capsaicin application produced a clear inward current and an associated increase in current variance, both of which were reversed after a suitable period of capsaicin washout. In order to determine the properties of the current ascribable to the capsaicin-gated conductance we subtracted sweeps recorded under control conditions from equivalent sweeps recorded in the presence of 30 μM capsaicin. The outcome of such a subtraction, from the sub-region of the trace surrounding and including the voltage ramp, is shown below the raw data traces in Fig. 2*A*. This trace indicates that the capsaicin-gated current is inward and non-desensitizing at −70 mV, but reverses polarity and exhibits significant outward rectification under the influence of a depolarizing voltage ramp. Using the ramp responses we were able to characterize the voltage dependence of the rVR1-mediated capsaicin-gated current. Figure 2*B* shows pooled normalized data derived from six voltage-ramp data sets, including that shown in Fig. 2*A*. It demonstrates that the reversal potential of the rVR1-mediated current is very close to 0 mV and that the response exhibits substantial outward rectification. The same data converted into a conductance–voltage plot are shown in Fig. 2*C*. This conversion was produced through the use of the interpolated reversal potential of each recording. For applications of 30 μM capsaicin the reversal potentials averaged +1·1 ± 0·7 mV ($n = 6$).

We next performed similar experiments to those shown in Fig. 2*A* but this time using reversed voltage ramps. In the first series of experiments, the cell was stepped to +70 mV for 100 ms before being ramped back down to −70 mV. In order to create a true 'mirror image' of the depolarizing ramp protocol described above, the hyperpolarizing ramp was applied at the same rate as ramps shown in Fig. 2*A*. With this protocol very similar current rectification was observed in a number of cells. As an illustration of this near identity of response, Fig. 2*D* compares normalized current–voltage relationships from the same four cells on which both depolarizing and hyperpolarizing ramp protocols were examined.

Additional experiments using 1 μM capsaicin revealed that the rectification properties of rVR1-mediated responses appeared to be independent of agonist concentration. We analysed the data to see if the degree of rectification in the rVR1-mediated responses to capsaicin (1 or 30 μM) depended in any way on the amplitude of the capsaicin-evoked current. To do this we used a simple index of rectification, namely the ratio of capsaicin-induced current at −70 mV and +70 mV ($I_{+70}/I_{-70\,\mathrm{mV}}$). When plotted against the amplitude of the capsaicin response recorded at −70 mV, no significant differences were observed between 1 and 30 μM capsaicin-evoked currents (Fig. 1*E*; mean rectification ratios were 4·4 ± 0·4 and 3·6 ± 0·6 and correlation coefficients (r) relating rectification ratio to current magnitude were −0·49 and −0·31 for responses to 1 and 30 μM capsaicin, respectively). The interpolated reversal potentials were also similar: +2·9 ± 1·6 ($n = 15$) and +1·1 ± 0·8 mV ($n = 25$) for currents evoked with either 1 or 30 μM capsaicin, respectively.

Voltage-dependent rectification properties of rVR1: negative slope conductance with strong hyperpolarizations

We also carried out experiments utilizing hyperpolarizing ramps to negative potentials beyond the normal holding potential of −70 mV. For these experiments, we used a ramp protocol from +70 to −200 mV. In the absence of capsaicin this hyperpolarizing ramp activated a small inward current, probably reflecting the activity of an inwardly rectifying K^+ channel in the HEK 293 cells. In the presence of capsaicin, the current waveform observed during the ramps suggested significant reduction of rVR1-mediated conductance at potentials more negative than −70 mV (Fig. 3*A*). This was confirmed by subtractive isolation of capsaicin-mediated currents from a number of similar experiments. Pooled normalized current–voltage data from six such recordings are shown in Fig. 3*B*. These demonstrate a region of clear negative slope conductance in the current–voltage relationship. Given the blocking effect of divalent cations such as Ba^{2+} and Mg^{2+} on various other

relationships constructed from cells to which both depolarizing (−70 to +70 mV) and 'mirror-image' hyperpolarizing (+70 to −70 mV) voltage ramps were applied at 0·14 mV ms^{-1}. Prior to applying the hyperpolarizing ramp the membrane potential was stepped to +70 mV (from −70 mV) for 100 ms. The pooled normalized current–voltage relationships shown were compiled as described in *B* from four cells. *E*, the relationship between current rectification ratio ($I_{+70}/I_{-70\,\mathrm{mV}}$) and the current magnitude ($I_{-70\,\mathrm{mV}}$) for current–voltage relationships determined for responses to 1 or 30 μM capsaicin.

channels, we were concerned that the region of negative slope conductance may have arisen from a voltage-dependent block of rVR1 by the Ba^{2+} present in our bathing solution. However, a similar region of negative slope conductance was also seen when we replaced extracellular Ba^{2+} with Ca^{2+} (Fig. 3*C*) and was also apparent in recordings in solutions in which divalent cations were nominally absent (Fig. 3*D*), suggesting that ionic block by external divalent cations was not occurring

Time-dependent properties of rVR1

Two aspects of the traces shown in Figs 2 and 3 point towards a non-instantaneous component of rVR1 rectification. The first is the exponentially rising component of capsaicin-evoked current observed when the membrane potential was stepped from −70 to +70 mV (Fig. 3*A*, arrow). The second is the 'tail current' seen on repolarization from +70 to −70 mV (Fig. 2*A*, arrow). Having observed these indicators of time-dependent gating we decided to characterize the kinetic aspects of rVR1 voltage dependence in more detail. To do this we performed experiments analogous to those in Fig. 2, but instead of voltage ramps we utilized voltage steps of various amplitudes and durations. As before, these voltage protocols were applied before, during and after application of 30 μM capsaicin and the properties of the net capsaicin-induced current were isolated by subtraction of the current response prior to capsaicin application from that observed at maximal steady-state rVR1 activation.

An example of an experiment in which voltage steps to four different potentials were applied for 300 ms is shown in Fig. 4*A*. The net capsaicin-induced current derived from this experiment is shown in Fig. 4*B*. It is clear that the current displays time-dependent properties. An exponentially rising component of current was observed following the initiation of depolarization and an exponentially decaying 'tail current' was observed on repolarization to −70 mV. The fact

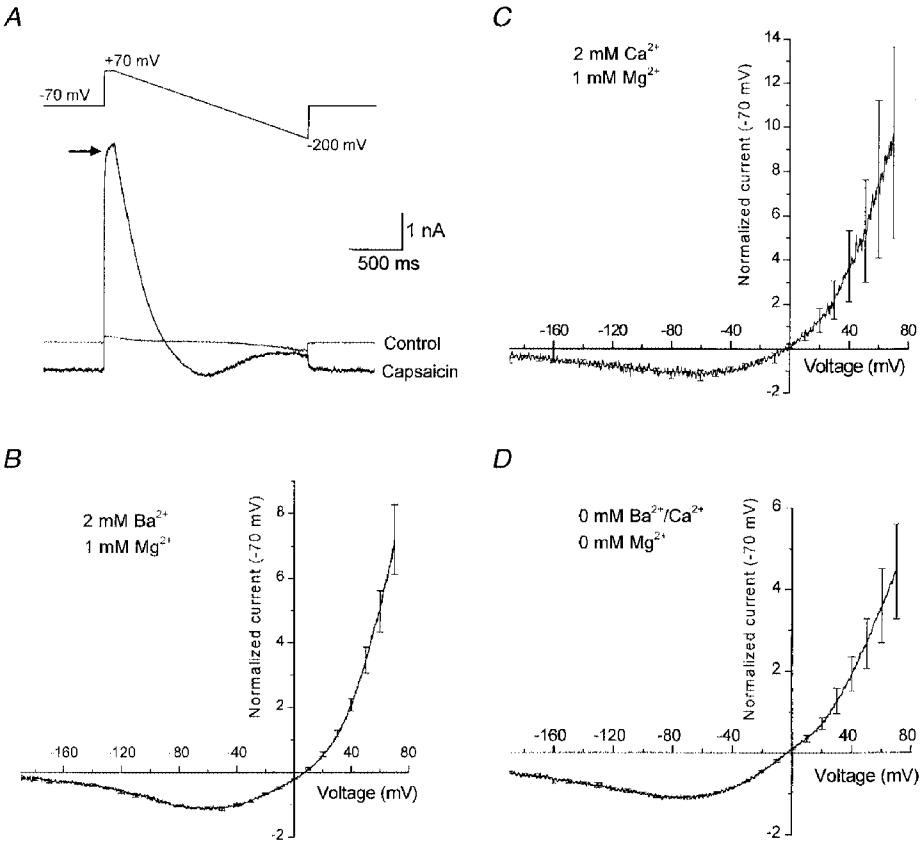

Figure 3. A region of negative slope conductance in the rVR1 current–voltage relationship

A, raw data traces from a whole-cell recording in which an extended hyperpolarizing voltage ramp was applied. The upper panel shows the voltage protocol used in which, after a period at −70 mV, the membrane potential was stepped to +70 mV for 100 ms; following this a ramp from +70 to −200 mV at 0·14 mV ms^{-1} was applied. Traces recorded prior to (Control) and during the steady-state phase of a capsaicin response (Capsaicin) are shown. Note the non-instantaneous rise in capsaicin-gated current seen when the membrane potential was stepped to +70 mV (arrow). *B*, the mean current–voltage relationship constructed from six recordings similar to and including that shown in *A*. Note the region of negative slope conductance observed at more negative potentials than −70 mV. *C*, the effect of replacing 2 mM Ba^{2+} with 2 mM Ca^{2+} on the rectification properties of rVR1. *D*, the effect of removal of extracellular divalent cations on the rectification properties of rVR1.

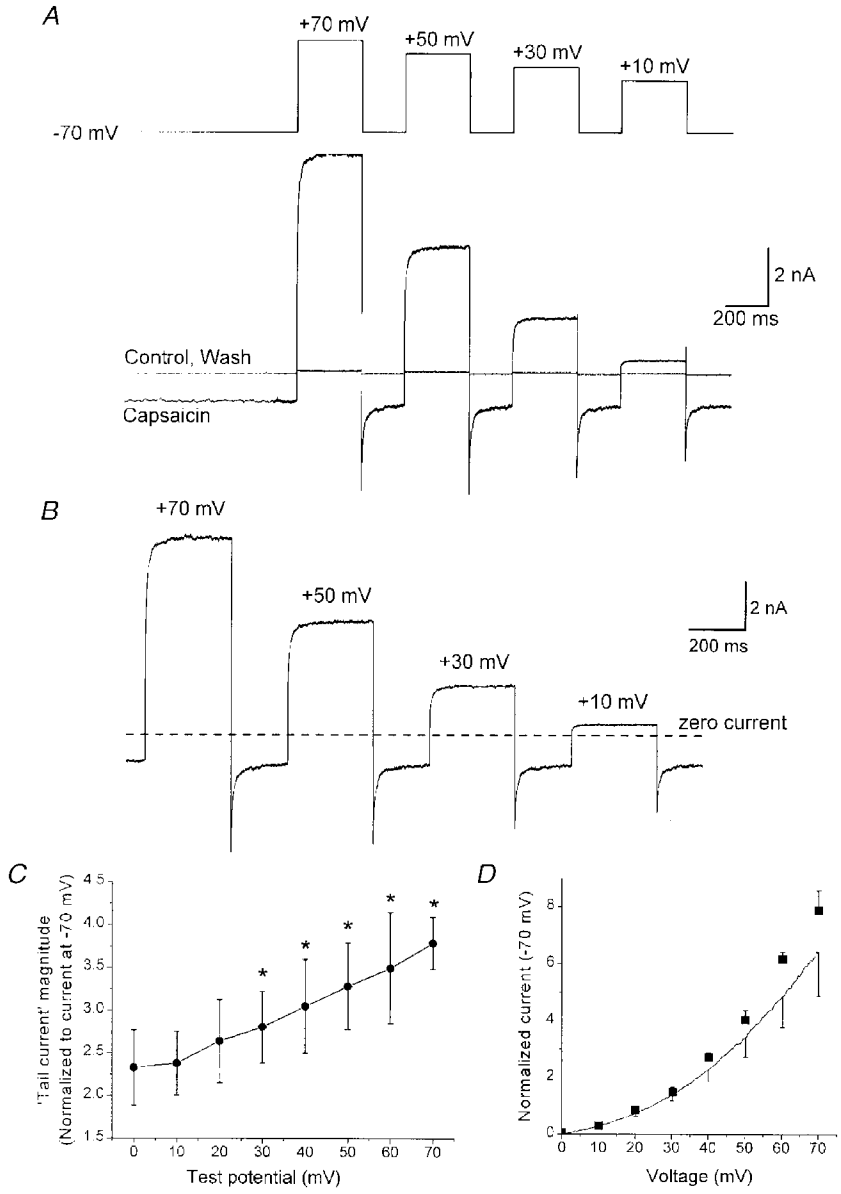

Figure 4. A time-dependent component of rVR1 rectification

A, a representative whole-cell recording of a typical cell showing the currents recorded in response to a voltage-step protocol (upper trace) applied in both the presence and absence of 30 μM capsaicin (lower traces). The voltage protocol contains a sequentially applied series of step depolarizations to +70, +50, +30 and +10 mV, each of 300 ms duration; similar data were also collected for voltage steps to +60, +40 +20 and 0 mV (not shown). *B*, the net capsaicin-gated component of the current subtractively isolated from the traces shown in *A*. Following steps in membrane potential, clear time-dependent current components were induced over and above those instantaneous current changes that simply arose through the enforced alteration in electrochemical driving force. These were manifest by the exponentially rising outward current seen following a depolarizing step and the overshooting inward 'tail current' observed following repolarization of the membrane to −70 mV. *C*, graph comparing the magnitude of the 'tail currents' observed at −70 mV following step depolarizations to test potentials between 0 and +70 mV. The data shown are from four cells and were normalized to the steady-state capsaicin-evoked current at −70 mV. * Significant difference ($P < 0{\cdot}05$, Student's paired t test) from a test depolarization to 0 mV. *D*, comparison of rVR1-mediated current–voltage relationships generated from depolarizing voltage-step and voltage-ramp protocols. The symbols plot the maximal rVR1-mediated response elicited by each level of test depolarization in experiments similar to that described in *A* and *B*. The data are normalized to the steady-state capsaicin-induced current seen at −70 mV. The line and error bars are replotted from the voltage-ramp data shown in Fig. 2*B*. The slightly lesser level of outward rectification in the data set from voltage ramps presumably reflects the inability of a ramp applied at 0·14 mV ms^{-1} to completely facilitate rVR1-mediated conductance.

that similar effects were observed in solutions which were nominally free of divalent cations suggests that a mechanism involving simple ionic block is unlikely to be responsible. Therefore, unlike the current responses of typical ligand-gated channels which exhibit instantaneous voltage-dependent properties (Hille, 1992), rVR1 appears to exhibit non-instantaneous rectification behaviour. A consequence of this is that rVR1 produces current waveforms with kinetic properties that are reminiscent of those that arise from voltage-gated K^+ channel activation and deactivation and implies that the rVR1 receptor protein may contain a voltage-sensitive domain.

If we assume that the effect of depolarization is to remove either inhibition of rVR1 or to exert a positive effect on the channel conductance then the decay of the 'tail' in the capsaicin-induced current observed on repolarization of the membrane to −70 mV probably reflects the re-establishment of the initial 'inhibited' state of the channel. Removal of this 'inhibition' at positive potentials may be what is responsible for the rectification profile of rVR1 as characterized in Figs 2 and 3. In fact, the exponential rise of current seen on depolarization is likely to reflect the kinetics of relief from this inhibited state at positive potentials. By measuring the amplitude of the tail current it is possible to probe the degree to which different test depolarizations relieve the inhibition of rVR1. With a depolarization to 0 or −10 mV the peak of the tail current at −70 mV was about 2·25-fold greater than the steady-state current observed at −70 mV, indicating a significant effect of 300 ms steps to holding potentials near the rVR1 current reversal potential. Increasing the level of the depolarization produced increasingly large repolarization-induced tail currents (Fig. 4*C*). This parallels the ongoing increases in conductance we observed as the membrane potential was moved in an increasingly depolarized direction (Fig. 2*C*).

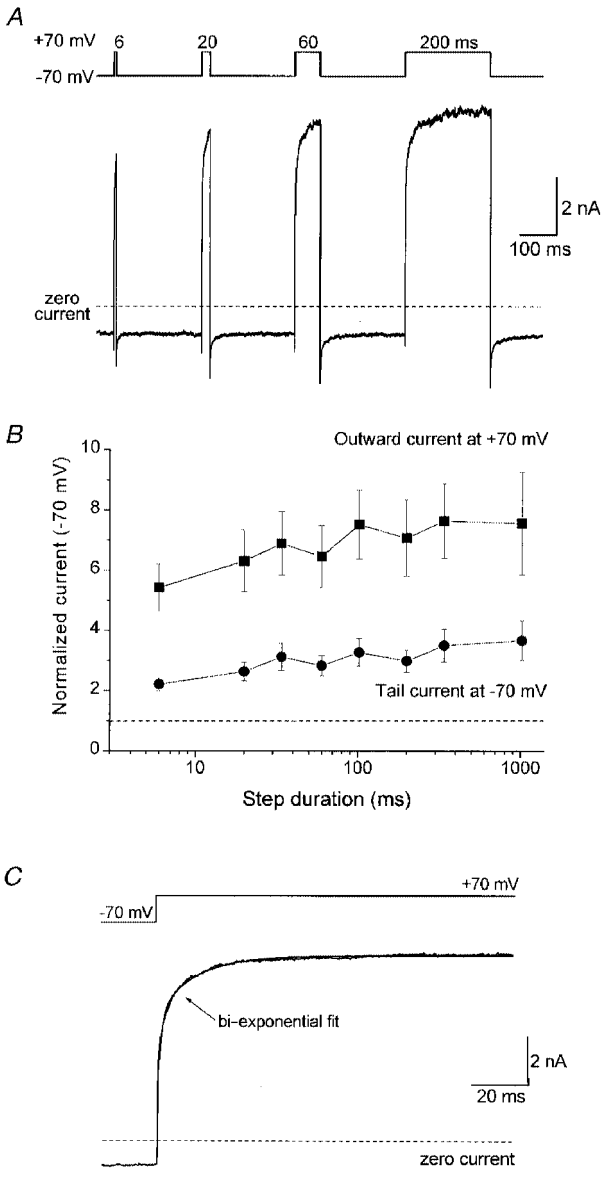

Figure 5. Activation kinetics of the time-dependent component of rVR1 rectification

A, a representative experiment conducted on a single capsaicin-responsive cell to determine the effect of the duration of membrane depolarization on the magnitude of the time-dependent component of rVR1 rectification. The voltage protocol (upper trace) used consisted of a series of step depolarizations to +70 mV of the following lengths: 6, 20, 60 and 200 ms. The current trace (lower panel) shows subtractively determined capsaicin-gated currents from a typical cell (subtraction was performed as described for the voltage ramps in Fig. 2). Additional data were also collected for step depolarizations of duration 34, 102, 340 and 1020 ms (not shown). *B*, a graph plotting the effect of increasing step duration on the maximum amplitude of outward current recorded at +70 mV and the magnitude of the 'tail current' observed following repolarization to −70 mV. The data shown are pooled from experiments performed on four cells. *C*, an example trace to illustrate on an expanded time course the activation kinetics of the outward current recorded in response to a depolarizing step from −70 to +70 mV. The non-instantaneous current component was best fitted by a bi-exponential function of time constants 6·7 ± 0·7 and 51·8 ± 18·4 ms with the faster time constant giving rise to 64·4 ± 3·8 % of the total current amplitude. Similar results were obtained for step potentials to other potentials (see text) indicating little or no voltage dependence of this event.

We also used the data obtained from these experiments to characterize the steady-state current–voltage relationship of rVR1. We measured the amplitude of the capsaicin-induced currents at the end of each depolarizing step and normalized this to the current observed in the steady state at −70 mV; a plot of these data *versus* holding potential is shown in Fig. 4*D*. Also shown on this graph is the mean current–voltage relationship replotted from Fig. 2*B*. This graph like those shown in Fig. 2 indicates that the average capsaicin-induced current at +70 mV was almost eight times larger than that at −70 mV. Although the curves generated with voltage step and ramps almost parallel each other, there is slightly less outward rectification in the data set obtained using voltage ramps. This presumably reflects the influence of the time-dependent properties of rVR1 on the ability of a ramp applied at 0·14 mV ms^{-1} to produce a true measure of the peak rVR1-mediated conductance at positive potentials.

Kinetic analysis of the time-dependent properties of rVR1

To characterize the kinetics of the time-dependent properties observed for rVR1 further we used two approaches. Firstly, we applied depolarizing voltage pulses to +70 mV with durations between 6 and 1020 ms and secondly, we analysed the kinetics of both the current waveforms in response to step depolarizations and those of the tail current events observed upon repolarization. Examples of capsaicin-induced currents in response to step depolarizations of varying length are shown in Fig. 5*A*. Analysis of the level of outward current induced by each step and the corresponding tail current amplitude are shown in Fig. 5*B*; as in previous experiments these current measurements were normalized to the steady-state capsaicin response observed at −70 mV. This analysis reveals that although a depolarizing pulse of around 100 ms may cause a maximal facilitatory effect on

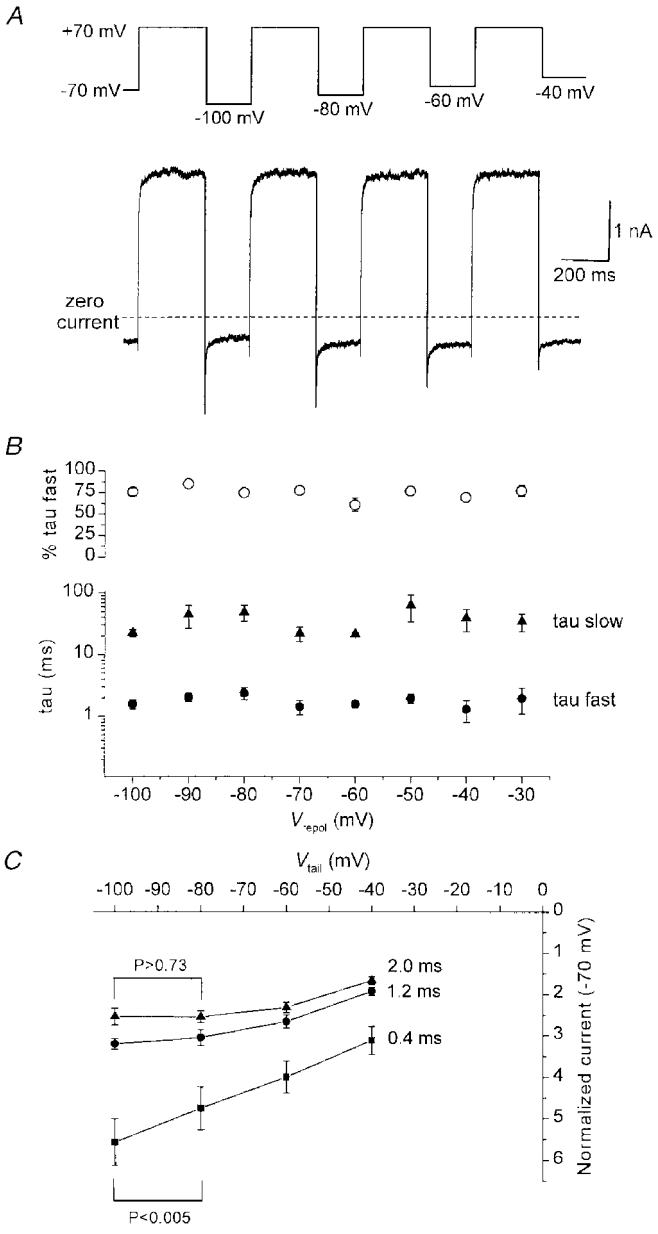

Figure 6. Kinetics and voltage dependence of rVR1-mediated tail currents

A, a representative experiment conducted on a single capsaicin-responsive cell to characterize the voltage dependence of rVR1-mediated tail current kinetics. The voltage protocol (shown in the upper trace) contains a series of step depolarizations (of 300 ms duration) to +70 mV followed by repolarization to a range of different membrane potentials. The current trace (lower panel) shows subtractively determined capsaicin-gated currents from a typical cell (subtraction was performed as described for the voltage ramps in Fig. 2). Similar data were also collected for repolarizations to −90, −70, −50 and −30 mV (not shown). *B*, kinetic analysis of the tail currents elicited by the range of repolarization potentials described in *A*. In all cells, at all potentials, the tail current trajectory was best fitted by a bi-exponential function. The graph plots, for each repolarization potential examined, the mean value of the two time constants associated with these fits (filled symbols) and the proportion ascribed to the faster component (○). *C*, a graph plotting current–voltage relationships for tail current amplitudes produced by step repolarizations from +70 to −100, −80, −60 and −40 mV. The three lines show representative data taken at time points 0·4, 1·2 or 2·0 ms after the initiation of the repolarizing step. Note the near linear current–voltage response observed at a latency of 0·4 ms and the rectifying one at 2·0 ms. Student's paired *t* test was used to compare the current amplitudes at −100 and −80 mV for post-repolarization latencies of 0·4 or 2·0 ms: a significant difference was present between the −100 and −80 mV current amplitudes at 0·4 ms ($P < 0·005$) but not for the equivalent comparison at 2 ms ($P > 0·73$).

rVR1, a substantial proportion of the increased response is seen with a 6 ms depolarization to +70 mV. This suggests that both fast and slow kinetic components are present and therefore suggests that a complex multi-step mechanism may underlie the depolarization-induced increase in conductance which we observe.

Kinetic analysis of the time-dependent component of the increase in rVR1 conductance in response to step depolarizations was performed by fitting exponential functions to individual current responses (Fig. 5*C*). This also revealed that the increase in rVR1-mediated conductance contained two clearly separable exponential components. For steps to +70 mV, these exponentials had mean time constants of 6·7 ± 0·7 and 51·8 ± 18·4 ms. The majority of the time-dependent conductance change (64·4 ± 3·8 %) arose from the faster of these two time constants. Similar bi-exponential rises in capsaicin-gated current were elicited by steps to other positive membrane potentials. Comparison of the kinetics for voltage steps to membrane potentials between +20 and +70 mV demonstrated that the two time constants underlying the rVR1 conductance increase appeared broadly similar across the range of potentials examined.

We also investigated the kinetics of the recovery of the tail current observed upon repolarization of the membrane following a depolarizing step. To look at this specifically, and to examine the possibility of voltage dependence of this event, we performed experiments (Fig. 6) in which a step to +70 mV was followed by repolarization to a range of different membrane potentials between −30 and −100 mV. An example of a typical recording for tail current analysis is shown in Fig. 6*A*. We characterized the kinetics of the recovery of the tail current recorded at each of the eight repolarization potentials and these data are plotted in Fig. 6*B*. From these experiments it is clear that the kinetics of the tail current recovery are described by a bi-exponential process, without any significant voltage dependence, hence the time constants of around 2 and 30 ms at all repolarization potentials between −100 and −30 mV (Fig. 6*B*). Therefore, the time-dependent events upon depolarization and repolarization share broadly similar kinetics and may represent forward and reverse rates of the same mechanistic event.

Given the biphasic decay of the tail current produced on repolarization of rVR1-expressing HEK 293 cells we went on to characterize the current–voltage relationship of the tail current at a number of different time points following repolarization. At the peak of the tail current (0·4 ms after the initiation of repolarization), the relationship between repolarization potential and tail current amplitude was roughly linear. In contrast, some 1·6 ms later in the tail current trajectory, the same relationship clearly exhibited the negative slope conductance that typifies the steady-state current–voltage relationship of rVR1. This can be seen in Fig. 6*C* where current–voltage relationships taken at 0·4, 1·2 and 2·0 ms after membrane repolarization are plotted. Statistical analysis of the current amplitude at repolarization potentials of −100 and −80 mV revealed that the current at −100 mV was greater than that at −80 mV at the peak of the tail current. However, 2 ms after repolarization this was no longer the case: at this time the mean current at −100 mV was slightly smaller than that at −80 mV, although this was not statistically significant. This analysis reveals that the fast time constant of the tail current decay seems to correlate well with the recovery of a region of negative slope conductance in the rVR1 current–voltage relationship.

DISCUSSION

In this article we have drawn attention to some novel and potentially important time-dependent rectification properties of rVR1. Our data indicate that as well as exhibiting the activation properties of a ligand-gated channel, rVR1 also possesses time-dependent gating properties that are reminiscent of voltage-gated channels. When considered together with the recent report by Piper & Docherty (1999), in abstract form, of broadly similar properties of capsaicin-gated responses in cultured dorsal root ganglion (DRG) neurones, these findings may have important implications for the normal functioning of VR1 receptors *in vivo*.

Activation of rVR1 by capsaicin

Our initial characterization of recombinant rVR1 expressed in HEK 293 cells demonstrates that it possesses the expected properties of the previously cloned capsaicin receptor (Caterina *et al.* 1997; Tominaga *et al.* 1998). The Hill coefficient of $\geqslant 2$ suggests that two or more capsaicin molecules are required for receptor activation. In addition, the relatively slow activation kinetics and the delay observed between capsaicin application and channel gating are consistent with the requirement for the lipophilic capsaicin to cross the membrane bilayer to gain access to its binding site(s). Similar observations have been made for capsaicin responses in DRG neurones (Koplas *et al.* 1997) and recently, Jung *et al.* (1999), using a charged version of capsaicin which cannot permeate the membrane bilayer, demonstrated convincingly that capsaicin does indeed bind to a site (or sites) accessible via the intracellular compartment.

Rectification properties of rVR1

The rectification properties of rVR1 defined by the current–voltage and conductance–voltage relationships that we have constructed from various voltage-ramp and -step protocols are reminiscent of reports on the properties of capsaicin-gated currents in DRG neurones (Oh *et al.* 1996; Piper *et al.* 1999; Nagy & Rang, 1999), and more recently for the recombinant receptor itself (Caterina *et al.* 1997; Tominaga *et al.* 1998). We, like others, observe a large degree of outward rectification (approximately 4- to 6-fold on average) and a reversal potential close to 0 mV, the latter being consistent with the gating of a non-selective cation channel. Where our findings differ is in the identification of, firstly, a region of negative slope conductance at potentials more negative than −70 mV (a feature which has not been

generally noted by others perhaps simply due to the fact that the current–voltage relationship has not been extended to holding potentials much beyond −70 mV; but see results from studies on capsaicin-gated currents in DRG neurones by Piper *et al.* 1999). Secondly, we have identified voltage- and time-dependent properties of rVR1 which may underlie the rectification behaviour of the channel and have consequences for its functioning *in vivo* (see below). Previous reports for the recombinant receptor (Caterina *et al.* 1997; Tominaga *et al.* 1998) have not identified any time-independent behaviour of rVR1. Our data, however, are supported by the recent report of similar time-dependent properties of capsaicin-gated currents in DRG neurones (Piper & Docherty, 1999; Piper *et al.* 1999).

The region of negative slope conductance that we have identified could be due either to a voltage-dependent rVR1 gating mechanism or a voltage-dependent block of the channel, possibly by divalent cations, in a similar way to the widely reported Mg^{2+} block of NMDA receptors. However, removal of Ba^{2+} or Ca^{2+} and Mg^{2+} from the extracellular solution had little or no effect on the outward rectification or the region of negative slope conductance in the current–voltage relationship of rVR1 and argues against a mechanism of simple ionic block by these ions.

Outward rectification of rVR1 is also manifest at the single-channel level. Recordings of capsaicin- or heat-activated single-channel events in rVR1-transfected HEK 293 cells (Caterina *et al.* 1997; Tominaga *et al.* 1998) or capsaicin- or heat-activated currents in DRG neurones (Nagy & Rang, 1999) all show strong outward rectification. Furthermore, if the extracellular Ca^{2+} and Mg^{2+} are eliminated (in the outside-out patch configuration) the outward rectification remains (Nagy & Rang, 1999). It is therefore tempting to speculate that the rVR1 gating mechanism itself is voltage sensitive, and indeed, unpublished observations using single-channel recording of native VR1 in a thin-slice preparation of rat DRG are consistent with this interpretation (A. Scholz, personal communication).

Time-dependent behaviour of rVR1

We have shown that depolarization of cells expressing rVR1 causes a time-dependent increase in apparent rVR1-mediated conductance. This rectification behaviour develops in a bi-exponential fashion with the faster time constant (∼7 ms) accounting for the majority (∼65 %) of the observed change. The presence of two distinct time constants in our experiments differs from the observations of Piper & Docherty (1999) who report a single rising-time constant for the capsaicin-gated currents of native DRG neurones. The time-dependent changes in capsaicin-gated conductance in native DRG neurones were also much slower than those we report here. Thus, whereas for depolarizing stimuli, we found time constants of around 5 and 50 ms, Piper & Docherty (1999) report a single rising-time constant of 385 ms at +40 mV. The magnitude of these differences suggests that the time- and voltage-dependent properties of rVR1 may also be regulated by some factor or mechanism(s) intrinsic to DRG neurones and not present in HEK 293 cells. For example, the discrepancies between native and recombinant systems could result from the presence of additional VR subunits, splice variants, or regulatory proteins in native cells or from differences in post-translational modification such as phosphorylation. *In vivo*, such heterogeneity could potentially give rise to VR-expressing cells with markedly different response kinetics. However, further experiments will be needed to address these possibilities.

The time-dependent increase in capsaicin-gated conductance at positive potentials was also reported by the large 'tail current' that was consistently observed upon membrane repolarization. This current is analogous to a classical voltage-gated calcium channel tail current in that it represents the kinetics of relaxation of a channel population from an elevated conductance level to a basal one. The kinetics of the decline of these tail currents upon repolarization were of a similar order to the time-dependent events observed on depolarization. Hence the tail currents were best described by bi-exponential functions with time constants of around 2 and 30 ms. Interestingly, the re-establishment of the region of negative slope conductance seen at relatively negative membrane potentials may relate to the faster of the two time constants as the negative slope conductance is at least partially re-established within a few milliseconds following membrane repolarization. However, the presence of a significant slow component indicates that following membrane depolarization the activity of rVR1 could remain significantly potentiated for as long as 100 ms; in cultured DRG neurones the equivalent time constant is even greater (e.g. a single exponential of 270 ms at −100 mV; Piper & Docherty, 1999) and suggests that VR responses could be potentiated *in vivo* for substantial periods following depolarization.

In qualitative agreement with Piper & Docherty (1999), we find that the kinetics of the observed time-dependent behaviour both upon depolarization and repolarization exhibit very weak or no voltage dependence. This stands in contrast to the gating properties of most (but not all) voltage-activated channels, which typically exhibit strongly voltage-dependent activation and deactivation kinetics (Hille, 1992). An explanation for this observation will require further elucidation of the mechanisms underlying the time-dependent changes in rVR1 conductance we have described herein. The lack of strong voltage-dependent kinetics, however, is indicative that the voltage-dependent transition involved in the conductance change is not rate limiting. A possible mechanism, therefore, may involve a fast voltage-dependent conformational change that then permits or restricts the non- or weakly voltage-dependent association or disassociation of a pore blocking entity.

At the molecular level rVR1 is related to store-operated calcium channels and the transient receptor potential (TRP) channels of *Drosophila*, all of which are predicted to share the same membrane-spanning topology (Caterina *et al.*

1997). Although there is no significant sequence homology it is interesting to note that topologically rVR1 is also similar to the voltage-gated channel superfamily exemplified by the Kv class of K^+ channels; however, it is not yet known whether or not the rVR1 shares a similar quaternary structure. The rVR1 subunit is predicted to possess six membrane-spanning segments (S1 to S6) and have a pore-forming loop between S5 and S6. K^+ channels (as well as Na^+ and Ca^{2+} channels) have their primary voltage-sensing region in the S4 transmembrane segment. This is formed from a collection of positively charged amino acids positioned at regular intervals across the membrane. The rVR1 sequence does not contain a similar motif in S4, although charged residues are found in a number of transmembrane helices. Future structure–function studies on rVR1 may allow the identification of a similarly important motif in this family of receptors.

Physiological relevance of the voltage- and time-dependent behaviour of rVR1

Although the occurrence of a region of negative slope conductance in the rVR1 current–voltage relationship is consistent with rVR1 possessing voltage-dependent rectification properties, it seems that this is unlikely to bear any direct physiological relevance as it is only manifest at negative potentials beyond the normal resting potential of sensory neurones *in vivo*. The time-dependent behaviour has, in our view, a much greater potential for producing significant effects on the properties of sensory responses triggered by the activation of VR1; changes in membrane potential due to the activation of nearby VR receptors or even other ligand- or voltage-gated ion channels could enhance VR function.

For instance, *in vivo*, activation of rVR1 produces depolarization of sensory neurones and the entry of calcium ions (Heyman & Rang, 1985; Marsh *et al.* 1987; Wood *et al.* 1988; Bevan & Szolcsanyi, 1990; Oh *et al.* 1996; Zeilhofer *et al.* 1997). This latter effect will occur directly through rVR1 and indirectly through the depolarization-induced activation of voltage-gated Ca^{2+} channels. A rVR1-mediated sensory stimulus producing sufficient depolarization to elicit action potential firing could, via the time-dependent effects reported here, lead to a substantial enhancement of the activity of rVR1-mediated responses. For such an enhancement of VR1 function to occur *in vivo*, it would be essential for the waveform of the DRG neurone action potential, or indeed a train of action potentials, to be of a suitable duration to significantly activate the increase in rVR1 conductance seen at positive potentials. Interestingly, like nociceptive afferents *in vivo* (Rose *et al.* 1986; Ritter & Mendell, 1992), capsaicin-responsive DRG and trigeminal neurones have been reported to exhibit longer duration somatic action potentials (~4 ms) than their capsaicin-resistant counterparts (Ingram *et al.* 1993; Baumann *et al.* 1996) and furthermore, capsaicin application typically produces robust trains of action potentials in responsive DRG neurones (Heyman & Rang, 1985; Baumann *et al.* 1996; Koplas *et al.* 1997). It therefore seems plausible that such stimuli would be sufficient to cause an enhancement of VR1 function. However, to place our observations fully into a physiological context, knowledge of both the time-dependent rectification properties of rVR1 at physiological temperatures and the waveform of the action potential at sensory terminals will be required.

The time-dependent rectification properties of rVR1 and the native capsaicin receptors of DRG neurones also suggest that these receptors are functionally capable of detecting synchrony between their own activation and action potential generation, and may perhaps report this coincidence through enhanced increases in intracellular Ca^{2+}. This is particularly interesting as any enhancement of Ca^{2+} entry could contribute to the local Ca^{2+}-dependent modulation of rVR1 function by Ca^{2+}-dependent enzymes such as calcineurin (Docherty *et al.* 1996; Koplas *et al.* 1997), or could contribute to facilitation of the release of inflammatory or sensory modulators (Bevan, 1996; Szolcsanyi, 1996) such as calcitonin gene-related peptide and substance P which are known to be co-expressed with rVR1 in some DRG neurones (Michael & Priestley, 1999).

The design of experiments to test the potential importance of the time- and voltage-dependent properties of VR1 is an interesting challenge for the future. It will be particularly important to test if the same time- and voltage-dependent properties are observed when VR1 is activated by its endogenous physiological activator(s); the list of candidates currently includes noxious heat, and/or increases in proton concentration (Cesare & McNaughton, 1996; Kress *et al.* 1996; Martenson *et al.* 1997; Caterina *et al.* 1997; Tominaga *et al.* 1998) and the endogenous lipid anandamide (Zygmunt *et al.* 1999; Smart *et al.* 2000).

Acklin, S. E. (1988). Electrical properties and anion permeability of doubly rectifying junctions in the leech central nervous system. *Journal of Experimental Biology* **137**, 1–11.

Baumann, T. K., Burchiel, K. J., Ingram, S. L. & Martenson, M. E. (1996). Responses of adult human dorsal root ganglion neurons in culture to capsaicin and low pH. *Pain* **65**, 31–38.

Baylor, D. A. & Nicholls, J. G. (1969). Chemical and electrical synaptic connexions between cutaneous mechanoreceptor neurones in the central nervous system of the leech. *Journal of Physiology* **203**, 591–609.

Bevan, S. (1996). Signal transduction in nociceptive afferent neurons in inflammatory conditions. *Progress in Brain Research* **113**, 201–213.

Bevan, S. & Szolcsanyi, J. (1990). Sensory neuron-specific actions of capsaicin: mechanisms and applications. *Trends in Pharmacological Sciences* **11**, 330–333.

Caterina, M. J., Schumacher, M. A., Tominaga, M., Rosen, T. A., Levine, J. D. & Julius, D. (1997). The capsaicin receptor: a heat-activated ion channel in the pain pathway. *Nature* **389**, 816–824.

Cesare, P. & McNaughton, P. (1996). A novel heat-activated current in nociceptive neurones and its sensitization by bradykinin. *Proceedings of the National Academy of Sciences of the USA* **93**, 15435–15439.

Collingridge, G. L. & Watkins, J. C. (ed.) (1994). *The NMDA Receptor*. Oxford University Press, Oxford.

Docherty, R. J., Yeats, J. C., Bevan, S. & Boddeke, H. W. (1996). Inhibition of calcineurin inhibits the desensitization of capsaicin-evoked currents in cultured dorsal root ganglion neurones from adult rats. *Pflügers Archiv* **431**, 828–837.

Goldman, D. E. (1943). Potential, impedance and rectification in membranes. *Journal of General Physiology* **27**, 37–60.

Heyman, I. & Rang, H. P. (1985). Depolarizing responses to capsaicin in a subpopulation of rat dorsal root ganglion cells. *Neuroscience Letters* **56**, 69–75.

Hille, B. (1992). *Ionic Channels of Excitable Membranes*. Sinauer, Sunderland, MA, USA.

Hodgkin, A. L. & Katz, B. (1949). The effect of sodium ions on the electrical activity of the giant axon of the squid. *Journal of Physiology* **108**, 37–77.

Ingram, S. L., Martenson, M. E. & Baumann, T. K. (1993). Responses of cultured adult monkey trigeminal ganglion neurons to capsaicin. *NeuroReport* **4**, 460–462.

Jung, J., Hwang, S. W., Kwak, J., Lee, S. Y., Kang, C. J., Kim, W. B., Kim, D. & Oh, U. (1999). Capsaicin binds to the intracellular domain of the capsaicin-activated ion channel. *Journal of Neuroscience* **19**, 529–538.

Koplas, P. A., Rosenberg, R. L. & Oxford, G. S. (1997). The role of calcium in the desensitization of capsaicin responses in rat dorsal root ganglion neurons. *Journal of Neuroscience* **17**, 3525–3537.

Kress, M., Fetzer, S., Reeh, P. W. & Vyklicky, L. (1996). Low pH facilitates capsaicin responses in isolated sensory neurons of the rat. *Neuroscience Letters* **211**, 5–8.

Lopatin, A. N., Makhina, E. N. & Nichols, C. G. (1994). Potassium channel block by cytoplasmic polyamines as the mechanism of intrinsic rectification. *Nature* **372**, 366–369.

Marsh, S. J., Stansfeld, C. E., Brown, D. A., Davey, R. & Mccarthy, D. (1987). The mechanism of action of capsaicin on sensory C-type neurons and their axons *in vitro*. *Neuroscience* **23**, 275–289.

Martenson, M. E., Arguelles, J. H. & Baumann, T. K. (1997). Enhancement of rat trigeminal ganglion neuron responses to piperine in a low-pH environment and block by capsazepine. *Brain Research* **761**, 71–76.

Michael, G. J. & Priestley, J. V. (1999). Differential expression of the mRNA for the vanilloid receptor subtype 1 in cells of the adult rat dorsal root and nodose ganglia and its downregulation by axotomy. *Journal of Neuroscience* **19**, 1844–1854.

Nagy, I. & Rang, H. P. (1999). Similarities and differences between the responses of rat sensory neurons to noxious heat and capsaicin. *Journal of Neuroscience* **19**, 10647–10655.

Nowak, L., Bregestovski, P., Ascher, P., Herbert, A. & Prochiantz, A. (1984). Magnesium gates glutamate-activated channels in mouse central neurones. *Nature* **307**, 462–465.

Oh, U., Hwang, S. W. & Kim, D. (1996). Capsaicin activates a nonselective cation channel in cultured neonatal rat dorsal root ganglion neurons. *Journal of Neuroscience* **16**, 1659–1667.

Piper, A. S. & Docherty, R. J. (1999). Capsaicin-activated currents in adult dorsal root ganglion (DRG) neurones in culture exhibit time-dependent behaviour. *Journal of Physiology* **518.P**, 118*P*.

Piper, A. S., Yeats, J. C., Bevan, S. & Docherty, R. J. (1999). A study of the voltage dependence of capsaicin-activated membrane currents in rat sensory neurones before and after acute desensitization. *Journal of Physiology* **518**, 721–733.

Ritter, A. M. & Mendell, L. M. (1992). Somal membrane properties of physiologically identified sensory neurons in the rat: effects of nerve growth factor. *Journal of Neurophysiology* **68**, 2033–2041.

Rose, R. D., Koerber, H. R., Sedivec, M. J. & Mendell, L. M. (1986). Somal action potential duration differs in identified primary afferents. *Neuroscience Letters* **63**, 259–264.

Smart, D., Gunthorpe, M. J., Jerman, J. C., Nasir, S., Gray, J., Muir, A. I., Chambers, J. K., Randall, A. D. & Davis, J. B. (2000). The endogenous lipid anandamide is a full agonist at the human vanilloid receptor (hVR1). *British Journal of Pharmacology* **129**, 227–230.

Szolcsanyi, J. (1996). Neurogenic inflammation: re-evaluation of axon reflex theory. In *Neurogenic Inflammation*, ed. Geppetti, P. & Holzer, P., pp. 35–44. CRC, Boca Raton, FL, USA.

Tominaga, M., Caterina, M. J., Malmberg, A. B., Rosen, T. A., Gilbert, H., Skinner, K., Raumann, B. E., Basbaum, A. I. & Julius, D. (1998). The cloned capsaicin receptor integrates multiple pain-producing stimuli. *Neuron* **21**, 531–543.

Wood, J. N., Winter, J., James, I. F., Rang, H. P., Yeats, J. & Bevan, S. (1988). Capsaicin-induced ion fluxes in dorsal root ganglion cells in culture. *Journal of Neuroscience* **8**, 3208–3220.

Zeilhofer, H. U., Kress, M. & Swandulla, D. (1997). Fractional Ca^{2+} currents through capsaicin- and proton-activated ion channels in rat dorsal root ganglion neurones. *Journal of Physiology* **503**, 67–78.

Zygmunt, P. M., Petersson, J., Andersson, D. A., Chuang, H., Sorgard, M., Di Marzo, V., Julius, D. & Hogestatt, E. D. (1999). Vanilloid receptors on sensory nerves mediate the vasodilator action of anandamide. *Nature* **400**, 452–457.

Acknowledgements

We would like to thank Dr Chris Benham and Professor Alan North for their comments on our initial experimental observations and Dr Andreas Scholz for allowing us to refer to details of unpublished work.

Corresponding author

M. J. Gunthorpe: Neuroscience Research, SmithKline Beecham Pharmaceuticals, New Frontiers Science Park (North), Harlow, Essex CM19 5AW, UK.

Email: Martin_J_Gunthorpe@sbphrd.com

Requests for materials should be addressed to J. B. Davis.

Email: John_B_Davis@sbphrd.com